EFFICIENT PHOTOVOLTAIC PUMP SYSTEM USING A PERMANENT MAGNET SYNCHRONOUS MOTOR DRIVE

S. Van Haute*, St. Henneberger*, K. Hameyer*, R. Belmans*
L. De Gheselle**, W.Coppye**, J. Nijs**

* Katholieke Universiteit Leuven, Belgium
** IMEC, Belgium

Abstract. In photovoltaic pump systems, the solar array accounts for a substantial fraction of the overall system cost. Therefore, all system components must have a high efficiency in a large power range. Low voltage standard induction motors do not fit this criterion. Hence, a dedicated 3.8 kW permanent magnet synchronous motor for a surface application is designed, built and compared to a standard induction motor. A damper cage is added to the permanent magnet rotor to allow open loop control. The motor is fed by a modified IGBT inverter, equipped with a selectable constant voltage or a maximum power point tracking facility. Furthermore, particular attention is paid to matching of all system components yielding maximum overall system performance. The system output in terms of pumped water is simulated for different geographical locations. Finally, the results of this test set-up are used to design a motor-pump unit suited for submersion.

Keywords. photovoltaic pump system, irrigation system, maximum power point tracking, permanent magnet motor

INTRODUCTION

Photovoltaic (PV) pump systems are used to provide drinking water and irrigation (Fig.1). Several systems have been developed in the recent past (Malbranche et al [1], Barlow et al [2], Makukatin [3]). Surface applications for irrigation systems are driven by permanent magnet dc machines while for submerged motor-pump units induction machines are used. However, small induction motors have, when compared with permanent magnet motors, a lower efficiency, whereas dc machines are not applicable for submerged installations.

Most of the currently operating photovoltaic systems offer a mechanical output power in the range of 0.85 kW up to 2.2 kW [1][3]. For higher system power ratings the cost of the photovoltaic array are increasing substantially. However, these larger systems offer major opportunities for increasing overall system efficiencies. As the cost of the photovoltaic array accounts for a substantial fraction (70 %) of the overall installed pump system cost [1], an increase in system efficiency can induce an important cost reduction. Although overall system efficiency is determined by the optimal matching of all system components (Fig. 2), increasing the efficiency of one component has a certain impact.

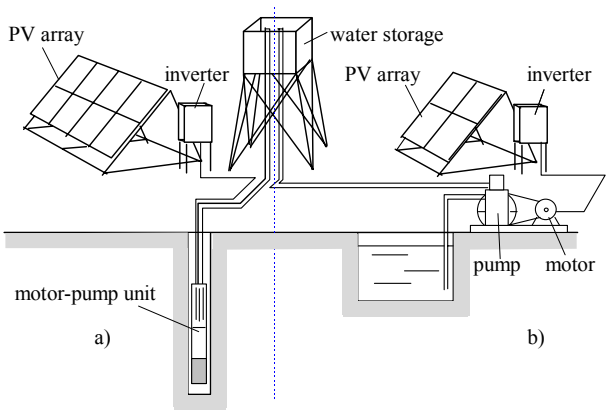

Figure 1: Photovoltaic pump systems: a) submerged motor pump unit and b) surface application.

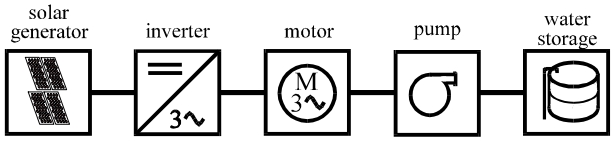

Figure 2: Main components of a photovoltaic pump system.

The total installed output power of the PV array for a given system yield in terms of daily pumped water is decreased using permanent magnet motors and is profitable for a relatively high system power rating. Therefore, a 3.8 kW permanent magnet synchronous motor (PMSM) is designed and developed for open loop control by implementing a damper cage. The design process combines analytical calculations with the finite element method (FEM). The motor is fed by a semi-standard inverter with selectable modes of operation. Experimental results from the drive are compared with the induction motor performance for a typical PV configuration.

PHOTOVOLTAIC ARRAY

The installed power and configuration of the photovoltaic array have to be designed in such a way that it is matched with the inverter, motor and pump obtaining a maximum water output volume under given meteorological conditions. The series and parallel connection of the photovoltaic modules is determined by the rated input power and allowed voltage range at the inverter input.

As an example, figure 3 shows the daily evolution of the global irradiation for the site of Bamako in Mali (12° N, 8.4° E) representative for the envisaged application circumstances of the system. The hourly meteorological data are generated based on average monthly values. A normalized 1 kWp PV array (10° tilt angle, south oriented) is simulated using a thermal model for free-standing modules and a one-diode electrical model. The histogram (Fig. 4) illustrates the distribution of time per year that a certain in-plane irradiation and module temperature occur at the PV array.

Based on this graph, water output calculations are performed and optimized for different system configurations. This will be described at the end of the paper.

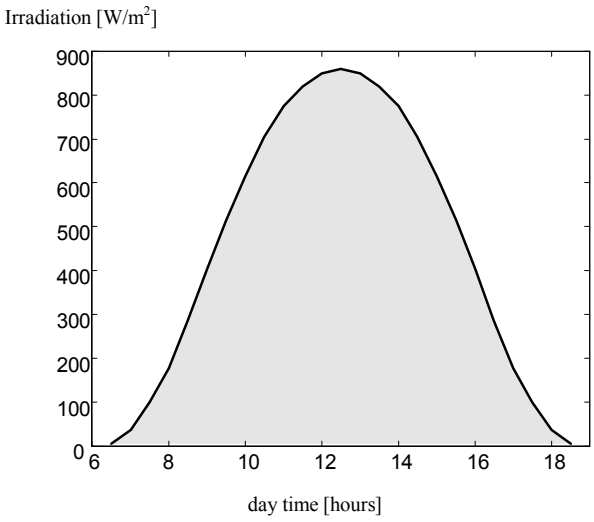

Figure 3: Distribution of the in-plane solar irradiation over the day (Bamako, Mali).

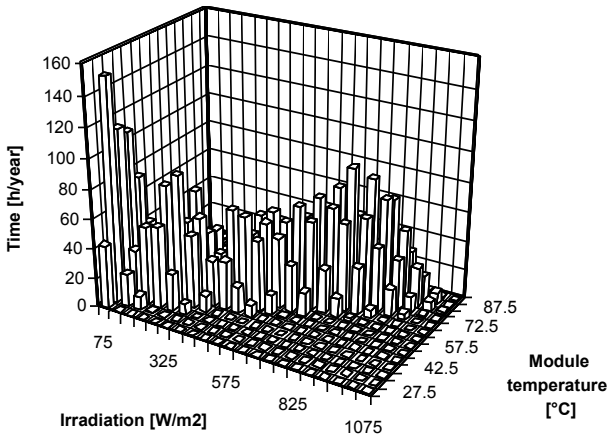

Figure 4: Distribution of the time per year irradiation and module temperature occur for a normalized PV system at Bamako (Mali)

For the motor with a rated power of 3.8 kW the optimal photovoltaic array has a peak power of 5.5 to 6 kWp. It is chosen to implement a rated PV array voltage of 270 V DC which corresponds to a rated motor voltage of 190 V. The higher voltage is chosen in order to limit the current. A high voltage reduces the motor size and the cost of the semi-conductor components for the inverter, as well as the inverter, losses and the conduction losses in the PV array. Special safety precautions have to be taken to apply this voltage without inducing higher personal risks.

According to the chosen DC voltage, several configurations are proposed and evaluated (Table 1). Using modules with larger power ratings results in less cabling and connecting costs. Each string consists of 18 modules.

TABLE 1 - Different PV configurations for the pump system

Module power (Wp)	Number of strings	Total peak-power (Wp)
70	5	6300
110	3	5940
120	3	6480

INVERTER AND SYSTEM CONTROL

Inverter type

No commercially available inverter for solar generators fulfils the combined requirements of the envisaged system, because of limited input voltage range, inverter standardization for induction motors and limited output frequency. However, the development and assembly of a completely new inverter would increase substantially the cost of the overall photovoltaic pump system. Therefore, a standard V/f controlled IGBT inverter is modified and adapted, adding a dedicated control algorithm and specific protection measures to ensure reliable operation under severe conditions. It is mounted on a water cooled backplane body and can be placed in an IP55 enclosure. Because of the use in rural environments, only a few relevant functions can be altered externally of the inverter after properly installing the system.

A wide DC voltage input range (100 V - 340 V) enables the use of the inverter in a variety of PV array configurations. During laboratory tests, the inverter was tested at different input voltages and under various load conditions. Its minimum efficiency is 95 %.

Input power control algorithm

As the pump system must have maximum performance, it is important that a suitable control algorithm is implemented. For the DC input power, three control schemes are proposed:

- constant voltage operation;
- constant voltage operation with feedback of the PV array temperature;
- maximum power point tracking.

Figure 5 illustrates the constant voltage operation mode and the MPP tracking mode. It shows typical I-V characteristics for one module at different levels of irradiation at constant cell temperature. In the constant voltage operation mode, the control algorithm forces the load to operate at a preselected DC inverter input voltage. This voltage (indicated by the vertical lines) can be chosen within a certain range to adapt a given PV array configuration.

Under ideal conditions and for an appropriate choice of the DC voltage (for example U_2), the constant voltage tracking can perform quite well. The vertical line is initially a good approximation of the real locus of maximum power points. As the I-V characteristics of the array shift horizontally with cell temperature, this straight-forward constant voltage tracking mode can be extended using cell temperature feedback. However, the output of the PV array is not maximized yet. Furthermore, voltage and temperature feedback properties have to be strictly adapted to the PV array. Assuming this

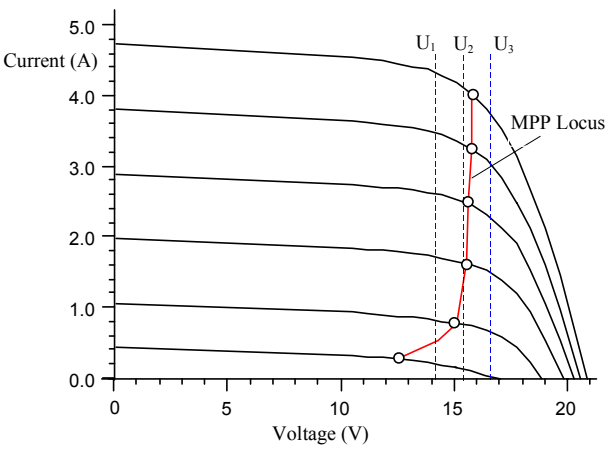

Figure 5: I-V characteristics with maximum power point locus and selected voltages for constant voltage operation (data for the 70 Wp modules used in the test array in figure 6).

during installation, this does not certify good performance throughout lifetime of the system.

Other effects such as partially shading (for example dust) and aging alter the PV array characteristics.

These two control algorithms are implemented by the manufacturer of the inverter. However, during laboratory tests on a real pump system, their performance was unsatisfactory.

It was considered necessary to work in the MPP at almost any time because the objective of the system is the maximization of the overall performance. This means that at each instant of time the PV array delivers its maximum available power to the motor. Therefore, to develop and test a MPP algorithm using a rapid prototyping set-up (dSPACE [6]), the same type of inverter was used with direct access to the firing circuits of the IGBT's. The control algorithm is programmed and downloaded using MATLAB®/SIMULINK® and the REAL TIME WORKSHOP® (dSPACE [7]). After satisfying testing, the algorithm is programmed in an EPROM and runs on the original prototype inverter.

The implemented continuous maximum power point tracking algorithm is based on simple decision rules, according to the I-V characteristics in figure 5. DC power is measured and compared to the previous measured value. When the power increases with increasing frequency, the frequencies further increased to maximize the power. When power decreases with increasing frequency, the set-point for the frequency should be lowered. For decreasing frequency the setpoint is further decreased when the power is increasing , but increases again when power decreases.

After laboratory tests with a DC voltage from a rotating generator, the algorithm is tested using a reduced PV array (Fig.6) and a portable induction motor-load unit.

Using this algorithm, effects of cell temperature, shadowing and aging, do not cause a mismatch of the PV array and inverter control characteristics. This makes the MPP tracking algorithm to be superior. Table 2 summarizes the results of a comparative simulation of the efficiency of the 3 algorithms for a normalized PV system under the given meteorological conditions. A difference of 2% in annual energy yields a trade-off hasannualto be considered between the increased system complexity and the additional PV module cost.

TABLE 2 - Normalized output for the site of Bamako in Mali

Algorithm	kWh/kWp
MPP Tracking	1661
Constant Voltage Tracking (CVT)	1636
CVT with T-feedback	1641

Figure 6: Photovoltaic array for testing the MPP algorithm (10 series connected 70 Wp modules).

Open loop V/f control

As the permanent magnet motor is controlled without position feedback, special attention has to be paid to the settings of the reference phase voltage at each speed. For a given pump, the required mechanical power is known from its characteristics. The induced voltage due to the permanent magnets is known as a function of speed and the terminal voltage minimizing the overall motor current can be calculated, based on the machine phasor diagram. This results in the optimal V/f characteristic for the inverter output.

MOTOR DESIGN

To obtain a maximum water output during one day, PV pump systems should reach a high conversion efficiency even at low irradiation levels (Fig. 3). This corresponds to the requirement to operate the motor with low losses in a large power range.

By studying the drive concept (Fig. 2), it is obvious that the motor is the only component where a relatively high improvement of the overall efficiency can be realized. Both the adaption of the motor to the pump as well as to the inverter is considered in order to obtain a high efficiency of the overall drive.

Permanent magnets

The high energy permanent magnet material NdFeB offers a high energy density ($BH_{max} \approx 300$ kJ/m^3). A high remanence flux density is recommended, while a high coercivity is less important as overloads do not occur using an inverter supply. Furthermore, motors operated with higher temperatures are no longer a drawback as the new generation of NdFeB magnets retains its magnetic properties up to high temperatures. Surface mounted magnet blocks, glued onto the rotor, reduce eddy current losses and thus the heating of the magnets.

PM rotor with additional damper cage

Besides the permanent magnets, the rotor carries a damper cage in order to enable the motor to operate in open loop control mode. Therefore, the angular magnet width is restricted to leave space for the rotor bars. The motor has a significant saliency and can be compared to a machine with surface-inset magnets (Nipp [8]). Figure 6 shows the rotor layout..

An advantage of the surface inset structure is that the torque giving force on the magnets is transferred to the rotor core by the iron between the magnets [9]. A disadvantage of this surface-inset type is the increased magnetic leakage flux at the permanent magnet edges.

The rotor bars are narrowing the flux path and thus saturation of the q-axis may occur. These saturation effects are computed using FEM. Figure 8 shows the flux plot of the magnetostatic solution of the PMSM under rated load conditions. The computed torque differs less than one percent from the analytical calculations. The calculated motor rated data are collected in Table 3.

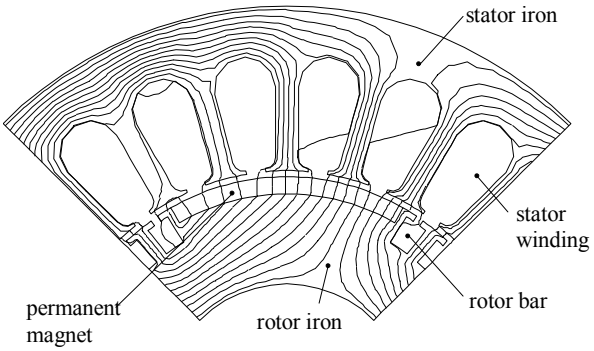

Figure 6: Flux lines of the PMSM at rated load.

TABLE 3 -Motor parameters

Motor parameter	Data
Number of poles	2p = 4
Rated speed	2240 rpm
Rated voltage	190 V
Rated current	14.8 A
Output power (at 2200 rpm)	3480 W
Torque	14.8 Nm
Efficiency	92.2 %

The efficiency at partial load is calculated using the equivalent circuit of the machine. As in irrigation systems no dynamic performance is required, a static solution is sufficient. The results are summarized in Table 4.

TABLE 4 -Motor performance

U	n	I	T_m	P_m	η
0.5 U_n	1068	I_n	16.13	1.80	87.24
0.6 U_n	1300	I_n	16.11	2.19	89.06
0.7 U_n	1533	I_n	16.10	2.58	90.36
0.8 U_n	1765	I_n	16.09	2.97	91.31
0.9 U_n	1998	I_n	16.07	3.36	92.05
1.0 U_n	2230	I_n	16.06	3.75	92.62
1.1 U_n	2463	I_n	16.04	4.14	93.07

Modified induction motor

In order to compare an induction motor to the PMSM, a 3.2 kW standard induction motor is modified by applying a new stator winding and a new rotor constructed as described in figure 6. The higher efficiency of the permanent magnet motor can be shown if the newly constructed rotor is compared to the original standard rotor of the induction machine, both having the same stator winding.

The experimental tests state a smooth start up of the drive as required and predicted. Measurements show that due to the new stator winding the point of maximum efficiency of the induction motor has shifted towards lower load regions (Fig. 8). However, the efficiency of the motor with the permanent magnet rotor is higher in the interesting torque range, when compared to the squirrel cage rotor. This means that for the same amount of pumped water, less PV modules are required.

PUMP LOAD AND SYSTEM EFFICIENCY

According to the envisaged installed power range, a centrifugal pump is chosen. Considering the constraints caused by the PMSM, the pump has the highest efficiency in the range of 1500 to 2200 rpm and a maximum mechanical power of 4 kW (Fig. 10). The optimum working conditions of the pump are found at a total manometric head between 12 and 18 m. However, this can be adapted by adjusting the impeller.

For a typical manometric head of 15 m, the inverter-motor-pump combination has an overall efficiency of more than 50 % between 1,5 and 4 kW mechanical output power with a maximum close to 60 %. During a long period of the day, the system is operating in this power range (Fig. 3). At very low power levels, the system efficiency deteriorates mainly due to the inevitable firm decrease of the pump efficiency (Fig.10).

More accurate results on (annual) water output for different geographical locations and system characteristics are obtained by an iterative calculation. Based on the data of figure 4 and the chosen tracking algorithm, the available DC power at different irradiation

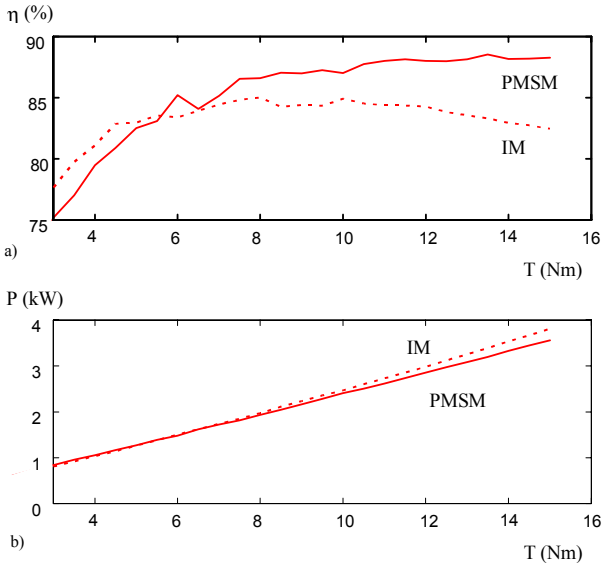

Figure 8: Comparison of experimental results of the permanent magnet and the squirrel cage rotor a) efficiency and b) output power versus torque.

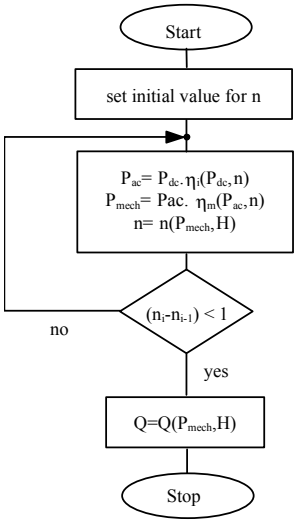

Figure 9: Iteration to calculate the water output of the system

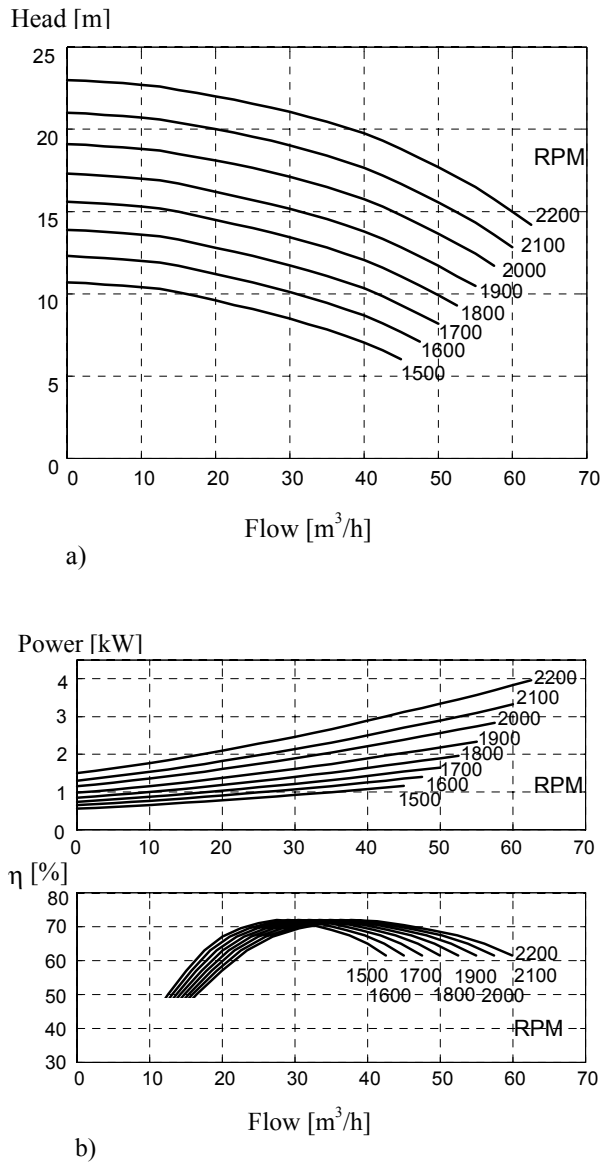

Figure 10: Pump characteristics:

a) flow rate as a function of the manometric head for different speeds
b) b) required power and efficiency as a function of the flow rate

levels is known. Because inverter and motor efficiency depend on the speed, the water flow is calculated using an iteration algorithm (Fig. 9) based on DC power, manometric head and pump characteristics. Integration results in the annual water output of a given system.

CONCLUSIONS

Measurements with a dedicated PMSM and inverter show that for larger PV pumping systems (3-4 kW) a substantial reduction of the required solar cells can be obtained, if all components are carefully matched. The PMSM motor design is applied to submerged applications in a cost-effective way, using standard components for housing, stator iron etc.

Acknowledgments

The research is supported by Flanders' Secretary of Economy. Furthermore, the authors are indebted to the Belgian Ministry of Scientific Research for granting the project IUAP No. P4/20 on Coupled Problems in Electromagnetic Systems.

References

1. Malbranche, Ph.; Servant J.M.; Hänel A.; Helm P.: Recent Developments in PV Pumping Applications and Research in the European Community, 12th European Photovoltaic Solar Energy Conference, 1994, pp. 476-481

2. Barlow, R.; McNelis, B.; Derrick, A.: Status and experience of solar PV pumping in developing countries, 10th European Photovoltaic Solar Energy Conference, 1991, pp. 1143-1146

3. Makukatin, S.:Water from the African sun, IEEE Spectrum, October 1994, pp.40-43

4. Nasar, S. A.; Boldea, I.; Unnewehr, L.E.: "Permanent Magnet, Reluctance, and Self-Synchronous Motors", CRC Press, London Tokyo, 1993.

5. Chang, L.; Dawson, G.E.; Eastham, T.R.: Permanent Magnet Synchronous Motor Design: Finite Element and Analytical Methods; ICEM '90, 1990, pp. 1082-1088.

6. dSPACE; 1993, Floating-Point Controller Board DS1102, User's Guide, Paderborn, Germany

7. dSPACE; 1995, Real-Time Interface to SIMULINK®,User's Guide, Paderborn, Germany

8. Nipp, E.; Alternative to Field Weakening of Surface Mounted Permanent Magnet Motors for Variable Speed Drives. Proc. IAS'95, pp. 191-198.

9. Sebastian T., Slemon, G. R., Rahman, M. A.; Design Considerations for Variable Speed Permanent Magnet Motors, Proc. ICEM'86, Sept. 1986, part 3 , pp. 1099-1102.

Address of the authors

S. Van Haute, St. Henneberger, K. Hameyer, R. Belmans,
Katholieke Universiteit Leuven,
E.E. Dept., Div. ESAT/ELEN,Kardinaal Mercierlaan 94, B-3001 Leuven, Belgium

L. De Gheselle, W.Coppye, J. Nijs
IMEC, Kapeldreef 75, B-3001 Leuven, Belgium